Using an ODE Solver for a Class of Integro-differential Systems

Alan C. Hindmarsh and Mark D. Rotter

Lawrence Livermore National Laboratory, Livermore, California 94551
E-mail: alanh@llnl.gov

By a simple extension of the Method of Lines, the ordinary differential equation solver VODPK may be used to solve a certain class of integro-differential equation systems (IDE systems). The problems are characterized by a pair of advected frequency-dependent quantities, coupled to a population variable whose rate includes a spectral integral in one space dimension. We have found that with an appropriate choice of preconditioner to aid in the convergence of the linear iterations, an extremely efficient method is obtained for the solution of these types of IDE system problems. We discuss the semidiscretization process and the formation of the preconditioner in some detail. Finally, we present an application of the technique.   © 2001 Academic Press

Key Words: integro-differential equations; Method of lines.

1. INTRODUCTION

The modeling of laser systems often requires computational models in which the intensities are functions of wavelength. The intensities and the laser level populations all vary with spatial position and with time. When the population rate equations involve an emission integral over the relevant spectrum, then the equations form a system of integro–differential equations (IDEs). We were faced with a problem of this sort, for which a one-dimensional spatial domain is sufficient to model a laser oscillator bounded by two mirrors. We began preparing a solution approach based on discretizing in space and frequency and using an ordinary differential equation (ODE) solver for the time integration—an approach that is highly successful for similar systems of time-dependent partial differential equations. In the process, it became apparent that the approach is valid for a somewhat more general class of 1D problems than for the laser oscillator in question. That class of problems is specified in the next section. The key feature is the coupling of two wavelength-dependent functions, representing physical quantities (e.g., intensities) that are advected in opposite

267

spatial directions, together with a third quantity (e.g., a population) driven by a spectral integral as well as other source terms. With the same formalism presented here, one can also solve considerably more general forms of IDE systems.

The use of a semidiscretized system (with time continuous) and an appropriate ODE algorithm for the time integration is called the Method of Lines [1] and is outlined for this problem class in Section 3. The method derives its power from the fact that problem-specific discretizations need only be done in space and (in this case) wavelength, while numerous powerful ODE solvers are available to carry out the time integration. The issue of time discretization errors is removed from the modeling effort, being reduced to the selection of tolerance inputs to the ODE solver. The use of the Method of Lines to solve IDEs is not new [2]. However, we believe the present treatment offers a significant advantage over previous methods in our choice of an efficient, stiff-ODE solver.

The ODE systems that arise here turn out to be *stiff*, meaning that they include one or more strongly damped (or rapid decay) modes, whose time scale is much shorter than the time scale of the solution itself. This stiffness necessitates the use of implicit methods for the integration of the ODE systems. However, the large problem size dictates the use of iterative methods for the linear systems that then arise. Then besides choosing a suitable ODE solver, success depends on providing a preconditioner to aid in the convergence of the linear iterative method. We have developed a product preconditioner for the stated class of problems, which has proven to be fairly simple to implement, and yet extremely effective in the solution. It is inspired by the idea of operator splitting, but does not sacrifice the critical element of error control. This preconditioner is developed in Section 4.

In Section 5, we present the application that led to this work. The specific problem of interest involves a laser with a solid-state gain medium. The laser cavity has a mirror whose reflectivity is a nonlinear function of the incident light intensity. The solid-state gain medium has a fluorescence decay time (200–300 μs) that is significantly longer than the time required for the radiation to build up inside the laser resonator. For this reason, this type of laser typically exhibits transient instabilities at the onset of oscillation, known as relaxation oscillations, which damp out as the lasing process proceeds. With a nonlinear mirror, the relaxation oscillation produces temporal spikes that can be significantly enhanced and do not damp out. There is interest in this type of resonator for a solid-state laser since a nonlinear mirror based on stimulated Brillouin scattering (SBS) can potentially provide the conjugation of the transverse modes of the counterpropagating radiation in the laser. Furthermore, the peak intensity enhancement provided by the nonlinear mirror could improve the laser's application in certain materials processing applications. A numerical model that helps tailor the design of the laser with respect to the peak output power and the temporal width and spacing of the output pulses would be a valuable tool. The solution of the problem follows the approach presented in the preceding sections, with some economies gained as a result of certain features of the semidiscrete problem. Solutions are shown for the simpler case with the nonlinear effect turned off, then with it turned on.

2. PROBLEM STATEMENT

We are interested in a system of integro-differential equations (IDEs) involving (as independent variables) one spatial variable x in an interval $x_L \leq x \leq x_R$, a wavelength λ, and time t. The dependent variables consist of two frequency-dependent quantities, y^+ and y^-, and a frequency-independent population, N. The quantities y^+ and y^- undergo

advection in the rightward and leftward directions (respectively) at a given speed v, and also reaction rates $R^{\pm}$. The rate equation for the population, N, includes a decay rate, S, which is an integral over wavelength of the sum $y^+ + y^-$, and a combinaton of other source and sink terms denoted P. More specifically, $y^+(x, \lambda, t)$, $y^-(x, \lambda, t)$, and $N(x, t)$ satisfy the following IDE system:

$$\partial y^+/\partial t + v\partial y^+/\partial x = R^+(y^+, N, \lambda) \tag{1}$$

$$\partial y^-/\partial t - v\partial y^-/\partial x = R^-(y^-, N, \lambda) \tag{2}$$

$$\partial N/\partial t = P(N, x, t) - NS[y^+ + y^-]. \tag{3}$$

The coefficient v and functions $R^{\pm}$ and S could also depend on x and t, but for brevity here, this dependency is not shown. Boundary conditions on $y^{\pm}$ are posed in which each is given as a function of the other at the appropriate endpoint, that is,

$$y^+(x_L, \lambda, t) = f_L[y^-(x_L, *, t)], \quad y^-(x_R, \lambda, t) = f_R[y^+(x_R, *, t)], \tag{4}$$

where each function f_L, f_R is an operator on the function $y^{\pm}$ that may involve its values at all wavelengths λ. To complete the problem statement, initial conditions $y^+(x, \lambda, 0)$, $y^-(x, \lambda, 0)$, and $N(x, 0)$ are to be given.

3. METHOD OF LINES APPROACH

The idea behind the Method of Lines approach to this IDE system is to discretize it in the space and wavelength variables, giving a system of ODEs in time that can be integrated by a suitable ODE solver. Specifically, suppose that a mesh of M intervals is placed on the x-interval, having the $M + 1$ meshpoints

$$x_L = x_0, x_1, \ldots, x_{M-1}, \quad x_M = x_R.$$

Likewise, discretize the wavelength interval into K points, as

$$\lambda_1, \ldots, \lambda_K.$$

Neither of these meshes need be uniform. At each point x_m and each wavelength λ_k we have discrete unknowns $y^+_{m,k}$ and $y^-_{m,k}$, and at each x_m we have an unknown N_m. At the interior mesh points ($0 < m < M$) we obtain an ODE for each $y^{\pm}_{m,k}$ by replacing the advection term in (1) and (2) by a suitable finite difference expression. For simplicity, we will use a simple two-point upwind difference here, although a more sophisticated discretization (possibly even of finite element type) could be used instead. Thus the ODEs from (1) and (2) are

$$dy^+_{m,k}/dt + v(y^+_{m,k} - y^+_{m-1,k})/\Delta x_{m-1} = R^+(y^+_{m,k}, N_m, t), \tag{5}$$

$$dy^-_{m,k}/dt - v(y^-_{m+1,k} - y^-_{m,k})/\Delta x_m = R^-(y^-_{m,k}, N_m, t). \tag{6}$$

To discretize the population equation (3), we must represent the integral operator S in terms of the discrete unknowns. For this we use the Trapezoid Rule, though a more

complicated quadrature could be used if needed. Thus in the case of a uniform wavelength mesh, we use

$$\int_{\lambda_1}^{\lambda_K} f(\lambda)\, d\lambda = \Delta\lambda \left[f(\lambda_1)/2 + \sum_{k=2}^{K-1} f(\lambda_k) + f(\lambda_K)/2 \right] \tag{7}$$

applied to the integrand f in the operator S. If the resulting value of S at x_m is denoted by S_m, then we have an ODE for N_m at each mesh point (including the boundaries) of the form

$$dN_m/dt = P(N_m, x_m, t) - N_m S_m. \tag{8}$$

Finally, the boundary conditions (4) become equations in the discrete variables of the form

$$y_{0,k}^+ = f_{Lk}(y_{0,1}^-, \ldots, y_{0,K}^-) \quad \text{and} \quad y_{M,k}^- = f_{Rk}(y_{M,1}^+, \ldots, y_{M,K}^+). \tag{9}$$

These equations complete the posing of Eq. (5) at $m = 1$ and of Eq. (6) at $m = M - 1$.

We now have a "semidiscrete" system, i.e., a set of ODEs in time which have been discretized in space and wavelength. This set consists of three subsets of the above equations, namely: (a) Eq. (5) for $m = 1, \ldots, M$; (b) Eq. (6) for $m = 0, \ldots, M - 1$; and (c) Eq. (8) for $m = 0, \ldots, M$. We write this system in a more compact form as follows. At the mth spatial point, define two vectors of size K,

$$y_m^\pm = (y_{m,1}^\pm, \ldots, y_{m,K}^\pm)^T.$$

Then at x_m we have a block of dependent variables,

$$y_m = (y_m^+, y_m^-, N_m)^T,$$

except that at the endpoints $m = 0$ and $m = M$ one of the two vectors $y_m^\pm$ is absent, by virtue of the boundary equations (9)

$$y_0 = (y_0^-, N_0)^T, \quad y_M = (y_M^+, N_M)^T.$$

The full dependent variable vector is

$$Y = (y_0, \ldots, y_M)^T. \tag{10}$$

Its size is $N = 2KM + M + 1$. The full set of ODEs can be written simply as

$$\dot{Y} \equiv dY/dt = F(t, Y). \tag{11}$$

The vector of initial values, $Y(0) = Y_0$, is given, and we seek the solution of the initial value problem on some time interval $0 \le t \le t_{max}$.

An important property of ODE systems that arises in this manner is "stiffness." An ODE system is stiff if it includes one or more rapid decay modes whose smallest time constant is very small compared to the time scale of the solution of interest. In discretized spatially dependent problems, stiffness often arises from the discretized spatial operator involved,

and it can also arise from the other rate terms present (such as $R^{\pm}$ here). This issue is important because if a nonstiff time integration method is used to solve a stiff system, it must be restricted to step sizes that are much smaller than necessary to resolve the solution accurately. The application given here is quite stiff, as we have learned by doing just such an experiment. In our case, the source of the stiffness can be traced to the advection terms.

The solutions also have oscillatory modes, which can take the form or periodic narrow spikes in time. But the time scales on which these spikes are resolved are still much longer than the time scale of the most rapid decay modes. The decay modes are absent in the solution, except for an initial fast transient, but their presence at all times in the ODE system itself makes it stiff.

Fortunately, a number of solver packages are available for the solution of stiff ODE initial value problems. Some are more suitable than others for the case of large systems that arise from PDEs or (as in this case) IDEs. The solver we have chosen is VODPK [3], a "Preconditioned Krylov" variant of the general-purpose solver VODE [4]. Our reasons for this choice will be made clear after the following short summary of these solvers.

Both of the solvers, VODE and VODPK, include two basic numerical methods for ODE systems (11). One is based on Adams–Moulton formulas and is useful only for nonstiff problems. The other is based on the backward differentiation formula (BDF) and is the one of interest here. Both are implemented in a variable-step-size, variable-order form. The BDF method uses the formulas

$$Y_n = \sum_{i=1}^{q} \alpha_{n,i} Y_{n-i} + h_n \beta_{n,0} \dot{Y}_n, \tag{12}$$

where the N-vector Y_n is the computed approximation to $Y(t_n)$. The step size (which can vary at every step) is $h_n = t_n - t_{n-1}$, and the coefficients $\alpha_{n,i}$ and $\beta_{n,0}$ are uniquely determined by the order q and the history of the step sizes. The integration begins with $q = 1$, and after that q varies automatically and dynamically between 1 and 5. Since $\dot{Y}_n$ denotes $F(t_n, Y_n)$, Eq. (12) is an implicit formula, and the nonlinear equation

$$G(Y_n) \equiv Y_n - h_n \beta_{n,0} F(t_n, Y_n) - a_n = 0 \tag{13}$$

must be solved for Y_n at each time step, where $a_n \equiv \sum_{i=1}^{q} \alpha_{n,i} Y_{n-i}$. For stiff problems, a Newton iteration is used to solve (13), and for each iteration an underlying linear system must be solved. This linear system for the Newton correction has the form

$$A\left[Y_{n(r+1)} - Y_{n(r)}\right] = -G\left(Y_{n(r)}\right), \tag{14}$$

where $Y_{n(r)}$ is the rth Newton iterate approximating Y_n, and

$$A = \frac{\partial G}{\partial Y} = I - \gamma J, \quad J \equiv \frac{\partial F}{\partial Y}, \quad \gamma \equiv h_n \beta_{n,0}.$$

An initial guess $Y_{n(0)}$ (also accurate to order q) is easily formed explicitly from past values Y_{n-i}. Depending on the particular method options chosen, the $N \times N$ matrix A may only be an approximation to $I - \gamma J$.

The integrator computes an estimate of the local errors at each time step, and strives to keep these below a certain tolerance. This error control uses a mix of relative and absolute

tolerance terms, where the tolerances themselves are supplied by the user. During the course of the integration, VODPK will vary both the step size h_n and the order q in an attempt to produce a solution with the minimum number of steps, but always subject to the local error test. See [4] for details.

The VODE solver uses only direct methods for the linear systems (14), and is precluded here because of the large size of our problems. In contrast, VODPK uses an iterative method, in which costs can be kept at a tolerable level by exploiting the structure of the problem. That iterative linear system method is based on the GMRES (Generalized Minimal Residual) Method [5], one of the so-called Krylov subspace iterative methods. The actual algorithm in VODPK is called SPGMR: Scaled, Preconditioned GMRES [6]. The user of VODPK may precondition the system on the left, on the right, or on both the left and right. Each value of the preconditioner is saved for repeated use over as many Newton iterations and as many time steps as possible. For similar problems in the past we have used LSODPK [6], an analogous preconditioned Krylov variant of the solver LSODE. But here we chose VODPK over LSODPK because the variable-step formulas underlying VODE and VODPK are likely to be more robust for these oscillatory problems than are the fixed-step-interpolate formulas in LSODE and LSODPK.

4. PRECONDITIONING

Although not required as input to VODPK, a preconditioner is usually necessary for efficiency in the solution of the linear systems (14) that arise, which we write here simply as $Ax = b$. A preconditioner is a matrix P that approximates A in some sense (possibly only crudely), but for which systems $Px = b$ can be solved reasonably efficiently. Given a preconditioner P, we apply the GMRES method either to the equivalent system $(P^{-1}A)x = P^{-1}b$ (for left preconditioning), or to the system $(AP^{-1})\,Px = b$ (for right preconditioning). In addition, we scale the iterative method, to account for differing orders of magnitude, and possibly different physical units, in the various components of the vectors x, etc. Here a diagonal matrix D is defined by way of tolerances supplied by the VODPK user, such that any error-like vector x is measured in terms of the weighted $L2$ norm $\|D^{-1}x\|_2$. Then in the SPGMR algorithm, the GMRES method is actually applied to the system $\tilde{A}\tilde{x} = \tilde{b}$ in which

$$\tilde{A} \equiv D^{-1}P^{-1}AD, \quad \tilde{x} \equiv D^{-1}x, \quad \tilde{b} \equiv D^{-1}P^{-1}b \text{ (left preconditioning)},$$

$$\tilde{A} \equiv D^{-1}AP^{-1}D, \quad \tilde{x} \equiv D^{-1}Px, \quad \tilde{b} \equiv D^{-1}b \text{ (right preconditioning)}.$$

The characteristic feature of a Krylov subspace method is that the system matrix is never needed explicitly, but only as an operator; that is, only its action on any given vector is needed. Thus the SPGMR method requires the action of the matrix $\tilde{A}$, or the value of matrix–vector products $\tilde{A}v$. The action of the factors D and D^{-1} is trivial. Using the relations $A = I - \gamma J$ and $J = \partial F/\partial Y$, we approximate the action of A by way of a difference quotient approximation,

$$Av = v - \gamma Jv, \quad Jv \approx [F(t, Y + \epsilon v) - F(t, Y)]/\epsilon,$$

for a suitably small ϵ. What remains is perhaps the most difficult part of the SPGMR method—defining and computing the action of P^{-1}, which means solving linear systems $Px = b$.

4.1. *Jacobian Structure*

To approximate $A = I - \gamma J$, a good preconditioner must include the numerically dominant contributions to the Jacobian J, but in a manner that permits efficient solution of the corresponding linear systems. To balance these two conflicting demands in the case of a large ODE system, it is essential to identify and exploit the sparsity structure of J. For the semidiscrete IDE systems here, J has contributions from the advective transport terms, the interaction terms on the right-hand side, and the boundary conditions. More specifically, writing

$$J = \partial(\dot{y}_0, \dot{y}_1, \ldots, \dot{y}_M)/\partial(y_0, y_1, \ldots, y_M),$$

we regard J in block form with $M + 1$ blocks in each direction, the dimension of each block being $2K + 1$ (in the interior) or $K + 1$ (at the edges). The diagonal blocks $J_m = \partial \dot{y}_m/\partial y_m$ each have a bordered-diagonal structure,

$$
J_m = \begin{pmatrix} J_m^{1+} & 0 & J_m^{2+} \\ 0 & J_m^{1-} & J_m^{2-} \\ J_m^3 & J_m^3 & J_m^4 \end{pmatrix} \quad (0 < m < M),
$$

$$
J_0 = \begin{pmatrix} J_0^{1-} & J_0^{2-} \\ J_0^3 & J_0^4 \end{pmatrix}, \quad J_M = \begin{pmatrix} J_M^{1+} & J_M^{2+} \\ J_M^3 & J_M^4 \end{pmatrix}.
\tag{15}
$$

Here J_m^{1+} and J_m^{1-} are diagonal matrices of size K with elements $\partial R^+/\partial y^+ - v/\Delta x_{m-1}$ and $\partial R^-/\partial y^- - v/\Delta x_m$. J_m^{2+} and J_m^{2-} are column vectors of size K with elements $\partial R^\pm/\partial N$. J_m^3 is a row vector of size K with elements $-N_m \partial S[y_m^{tot}]/\partial y_{m,k}^{tot}$. (The same row vector appears in two positions in J_m because S depends only on the sum $y_m^{tot} \equiv y_m^+ + y_m^-$.) J_m^4 is the scalar $\partial P(N_m, x_m, t)/\partial N_m - S_m$.

The off-diagonal blocks of J come from the advection terms and from the boundary equations. Those from the advection are diagonal matrices of size K,

$$A_m^+ = \partial \dot{y}_m^+/\partial y_{m-1}^+ \ (2 \le m \le M), \quad A_m^- = \partial \dot{y}_m^-/\partial y_{m+1}^- \ (0 \le m \le M - 2), \tag{16}$$

with elements $v/\Delta x_{m-1}$ and $v/\Delta x_m$. Those from the boundary equations (9) are matrices of size K,

$$B_L = \partial \dot{y}_1^+/\partial y_0^- = \frac{v}{\Delta x_0} \partial f_L(y_0^-)/\partial y_0^-, \quad B_R = \partial \dot{y}_{M-1}^-/\partial y_M^+ = \frac{v}{\Delta x_{M-1}} \partial f_R(y_M^+)/\partial y_M^+, \tag{17}$$

which may well have a nondiagonal structure.

4.2. *Forming a Preconditioner*

A natural and powerful way to form preconditioners for complex systems is to form a preconditioner for each of two or more parts of the problem, and multiply these together. The resulting *product preconditioner* is the product of matrices of the form $I - \gamma \tilde{J}$, in which each factor $\tilde{J}$ includes certain parts of J, and when added together the matrices $\tilde{J}$ include all of the numerically important contributions to J. This idea has been explored

extensively in [6] for the method of lines solution of reaction–transport PDE systems. For the present system, although there are many choices for the splitting of the Jacobian, we have made the specific choice

$$P = P_{advec} P_{border} = (I - \gamma J_{advec})(I - \gamma J_{border}), \tag{18}$$

where

- J_{advec} includes the advection contributions, an approximation to the boundary equation contributions, and the self-couplings $J_m^{1\pm}$, while
- J_{border} is a block-diagonal matrix with bordered-diagonal blocks consisting of the contributions $J_m^{2\pm}$, J_m^3, and J_m^4.

It is the factor J_{border} which includes the contribution of the spectral integral S in Eq. (3).

Since $P = I - \gamma (J_{advec} + J_{border}) + O(\gamma^2)$, and γ is proportional to the stepsize h_n, we can expect P to be a good approximation to $A = I - \gamma J$ at least for small enough stepsizes. In fact, we find that it performs very well for large stepsizes also. Further justification for this choice can be found by looking at the error term $\gamma^2 J_{advec} J_{border}$. For this, consider the problem with the dependent variables ordered as $\hat{Y} = (Y^+, Y^-, N)^T$, where each $Y^\pm$ consists of all the $y_{m,k}^\pm$, and N consists of all the N_m. Then the Jacobian takes the block form

$$\hat{J} = \begin{pmatrix} J_{11} & 0 & J_{13} \\ 0 & J_{22} & J_{23} \\ J_{31} & J_{32} & J_{33} \end{pmatrix}.$$

In this ordering, the chosen splitting corresponds to

$$\hat{J}_{advec} = \begin{pmatrix} J_{11} & 0 & 0 \\ 0 & J_{22} & 0 \\ 0 & 0 & 0 \end{pmatrix}, \quad \hat{J}_{border} = \begin{pmatrix} 0 & 0 & J_{13} \\ 0 & 0 & J_{23} \\ J_{31} & J_{32} & J_{33} \end{pmatrix}.$$

The product of these matrices,

$$\hat{J}_{advec} \hat{J}_{border} = \begin{pmatrix} 0 & 0 & J_{11} J_{13} \\ 0 & 0 & J_{22} J_{23} \\ 0 & 0 & 0 \end{pmatrix},$$

has nonzeros in only two of the nine block positions. This suggests (but does not prove) that the error in the corresponding product preconditioner may be smaller than for other splitting choices, which produce nonzeros in other blocks of the product.

For all of these Jacobian contributions, it is sufficient to use approximations to the true Jacobian elements, because of the way they are used within the GMRES iteration. Moreover, it can be highly beneficial to do this if the savings in computation and/or storage outweighs the increase in number iterations required for convergence. In our case, for example, it might be useful to replace the true value of the boundary equation Jacobian blocks B_L and B_R in (17) by sparse approximations to them, or to replace the diagonal terms $\partial R^\pm / \partial y^\pm$ by less costly approximations, depending on the complexity of the functions involved.

4.3. *Solving the Preconditioner Systems*

The solution of the preconditioner linear systems is split into two phases. First, we evaluate the factors of P and preprocess them in preparation for solving the linear systems later. Then each linear system $P_{advec} P_{border} x = b$ is solved, by solving two systems in succession, using the data saved from the preprocessing phase. The VODPK solver calls the routines that execute these two phases as needed, and it calls the (more expensive) preprocessing routine much less frequently than the solution routine.

For the block-diagonal matrix

$$P_{border} = diag\{B_0, B_1, \ldots, B_M\},$$

the preprocessing consists of performing an LU factorization of each block B_m. By construction, we have $B_m = I - \gamma J_{m,border}$, where $J_{m,border}$ is J_m with the diagonal pieces $J_m^{1\pm}$ removed. (We use I here to denote the identity matrix of the appropriate order, which may vary according to context.) This matrix actually has a *bordered-identity* form

$$B_m = \begin{pmatrix} 1 & & & a_1 \\ & \ddots & & \vdots \\ & & 1 & a_n \\ b_1 & \cdots & b_n & c \end{pmatrix}$$

of size $n + 1$ with $n = 2K$ or K. The LU factorization of this matrix is simply

$$B_m = \begin{pmatrix} 1 & & & \\ & \ddots & & \\ & & 1 & \\ b_1 & \cdots & b_n & 1 \end{pmatrix} \begin{pmatrix} 1 & & & a_1 \\ & \ddots & & \vdots \\ & & 1 & a_n \\ & & & c' \end{pmatrix} \quad \text{with } c' = c - \sum_1^n a_i b_i.$$

Solving a linear system $P_{border} x = b$ amounts to solving the blocks $B_m x_m = b_m$, which is easily done with backsolve operations using the saved LU factors.

For the factor P_{advec}, a block-LU treatment is possible, but for this it is helpful to look at a reduced and reordered form of the system. Note that J_{advec} does not involve the variables N_m at all. The corresponding equations in the system $P_{advec} x = b$ have the trivial form $x^i = b^i$ (using superscripts to denote components), and so we can drop those components from consideration. Also, because the couplings from advection are in alternate directions ($\dot{y}_m^+$ to y_{m-1}^+ and $\dot{y}_m^-$ to y_{m+1}^-), the structure of P_{advec} is greatly simplified if we consider, for the purposes of solving this system, the ordering

$$\bar{Y} = (y_1^-, y_2^-, \ldots, y_{M-1}^-, y_M^+, y_{M-1}^+, \ldots, y_1^+, y_0^-) \tag{19}$$

of the unknowns, instead of that in (10). With this ordering for both the b and x vectors, and the components corresponding to N_m dropped, the linear system $P_{advec} x = b$ takes the

form $\bar{P}_{advec}\bar{x} = \bar{b}$ with $\bar{P}_{advec} = I - \gamma \bar{J}_{advec}$ and

$$
\bar{J}_{advec} =
\begin{pmatrix}
J_1^{1-} & A_1^- & & & & & & \\
 & \ddots & \ddots & & & & & \\
 & & \ddots & A_{M-2}^- & & & & \\
 & & & J_{M-1}^{1-} & B_R & & & \\
 & & & & J_M^{1+} & A_M^+ & & \\
 & & & & & \ddots & \ddots & \\
 & & & & & & \ddots & A_2^+ \\
 & & & & & & & J_1^{1+} & B_L \\
A_0^- & & & & & & & & J_0^{1-}
\end{pmatrix},
\tag{20}
$$

in terms of the matrix blocks defined in Eqs. (15)–(17). This matrix $\bar{P}_{advec}$ is nearly a block-bidiagonal matrix, differing only in the presence of the corner block A_0^-. Such a matrix is called *bordered-block-bidiagonal*. For a general matrix of this form,

$$
H =
\begin{pmatrix}
D_1 & C_1 & & \\
 & \ddots & \ddots & \\
 & & D_{n-1} & C_{n-1} \\
C_n & & & D_n
\end{pmatrix},
\tag{21}
$$

a block-LU factorization can be easily performed, provided that all the D_j are nonsingular. The result is

$$
H =
\begin{pmatrix}
D_1 & & & \\
 & \ddots & & \\
 & & D_{n-1} & \\
E_1 & \cdots & E_{n-1} & E_n
\end{pmatrix}
\begin{pmatrix}
I & C_1' & & \\
 & \ddots & \ddots & \\
 & & I & C_{n-1}' \\
 & & & I
\end{pmatrix},
\tag{22}
$$

where the blocks in the factors are given by

$$
C_1' = D_1^{-1}C_1, \ldots, C_{n-1}' = D_{n-1}^{-1}C_{n-1},
$$
$$
E_1 = C_n, E_2 = -E_1 C_1', \ldots, E_{n-1} = -E_{n-2}C_{n-2}',
\tag{23}
$$
$$
E_n = D_n - E_{n-1}C_{n-1}'.
$$

In our case, $n = 2M$ in (21), and all the matrix blocks are $K \times K$. Furthermore, all the blocks in H are diagonal except possibly for $C_{M-1} = -\gamma B_R$ and $C_{2M-1} = -\gamma B_L$, and this fact can be exploited to reduce greatly the cost of the operations in (23). Once this block factorization is done, and provided also that the block E_n is nonsingular, solving a linear system $P_{advec}x = b$ reduces to block-backsolve operations in the blocks of b and x corresponding to the $y_m^\pm$. These can be carried out without any explicit reordering of the vectors, simply by observing the order of the blocks in (19).

5. AN APPLICATION

As an application of the formalism developed in this paper, we shall take an example from laser physics and model the behavior of a laser oscillator with a nonlinear mirror on one end. Such a situation is encountered when one constructs such an oscillator with a phase-conjugate mirror [7, 8]. These types of lasers are useful when it is desired to have an output beam free from aberrations caused by the laser medium, and usually the phase conjugation is achieved through a nonlinear process such as stimulated Brillouin scattering (SBS). To keep the application simple, we shall limit our model to a rate equation/intensity formalism.

5.1. Problem Statement

The geometry for the laser is shown in Fig. 1, where, for simplicity, we shall consider only one-dimensional propagation of the laser beam. The laser cavity itself has length L_c and the two (linear) mirrors defining the cavity have reflectivity R_{10} and R_2. All physics of the SBS process is grouped into an intensity and wavelength-dependent reflectivity, R_{11}, which is at the same location as R_{10}. The laser medium has a length L_a and is pumped uniformly in space at a time-dependent intensity I_p (W/cm^2). Within the cavity are circulating spectral intensities i_ℓ^+ (i_ℓ^-) (W/cm^2-nm), which move in the positive (negative) x-direction. In operation, laser oscillation builds up between the cavity mirrors R_{10} and R_2. Once the intensity builds up above a threshold for R_{11}, oscillation starts taking place between that mirror and R_2.

In SBS, light that gets reflected back into the cavity is wavelength-shifted by an amount equal to the Stokes shift of the SBS medium. Consequently, it is important to formulate the rate/transport equations describing the laser to explicitly take into account the wavelength dependence of the emission cross section. As a representative laser medium, we shall consider Nd-doped gallium gadolinium garnet (Nd:GGG), which has an emission wavelength of 1062 nm. To further simplify the analysis, we shall assume Nd:GGG acts as a four-level laser. In general, the decay times from the pump bands to the upper laser level, and from the lower laser level to the ground state, are at most a few nanoseconds (and typically much more rapid) [9]. Since the time scale of interest is on the order of 100 μs, we only need consider a rate equation for the upper laser level (which is directly populated by the pump).

In dimensional form, the rate and transport equations for $N_2(x, t)$ and $i_\ell^\pm(x, \lambda, t)$ read

$$\frac{\partial N_2}{\partial t} = \frac{\sigma_a N_0 I_p(t)}{h\nu_p} - \frac{N_2}{t_F} - \frac{N_2 \cdot 10^{-7}}{hc} \int_{emband} \lambda \sigma_s(\lambda)(i_\ell^+ + i_\ell^-)\, d\lambda,$$

$$\pm\frac{\partial i_\ell^\pm}{\partial x} + \frac{n}{c}\frac{\partial i_\ell^\pm}{\partial t} = \sigma_s(\lambda) N_2 [i_\ell^\pm + i_N^\pm(\lambda)](L_a/L_c) - \alpha i_\ell^\pm (L_a/L_c),$$
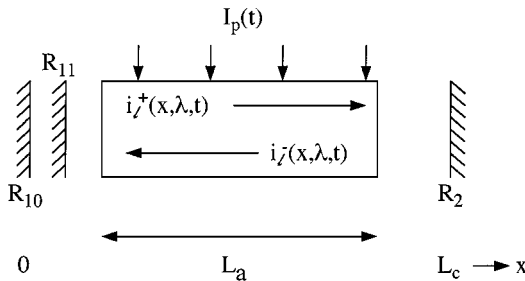
$$(24)$$

FIG. 1. Geometry for the laser.

where N_2 is the population of the upper laser level (cm^{-3}); N_0 is the population of the ground state (assumed constant, equal to the doping density); h is Planck's constant (J-s); ν_p is the pump frequency; σ_a and σ_s are the absorption and emission cross sections (cm^2); t_F is the fluorescence lifetime (s); $i_\ell^\pm$ are the forward and backward-going light spectral intensities (W/cm^2-nm); and n is the refractive index of the laser medium. The integral in the first equation is performed over the emission band. The factor 10^{-7} (cm/nm) allows us to express wavelengths in nm, while the spectral intensity has units W/cm^2-nm; L_a and L_c are the lengths of the active region and the cavity respectively (cm); and $i_N^\pm(\lambda)$ is the effective noise source (W/cm^2-nm), which initiates the lasing process. For the simple application given here, we shall take $i_N^\pm$ to be a constant, independent of position or wavelength. Finally, the factor α (cm^{-1}) represents any losses in the active medium.

In reality, there are many lines in the $^4F_{3/2} \rightarrow {}^4I_{11/2}$ transition in Nd:GGG [10]. However, to keep the application simple, we shall only consider the emission at 1062 nm in these calculations. The emission lineshape is taken to be a Gaussian with peak value σ_0 and FWHM $\Delta\lambda(=\sqrt{\ln 2} \approx 0.83$ nm):

$$\sigma_s(\lambda) = \sigma_0 \exp[-4\ln 2(\lambda - \lambda_0)^2/\Delta\lambda^2].$$

Instead of dealing with the dimensional form of Eqs. (24) directly, it is more useful to cast them in nondimensional form. The details of the nondimensionalization of the equations are given in the Appendix. In terms of a dimensionless coordinate ξ varying between 0 and 1, a dimensionless time τ, and a dimensionless wavelength Λ varying between Λ_ℓ and Λ_u, the normalized dependent variables are $\eta(\xi, \tau)$ and $y_\ell^\pm(\xi, \Lambda, \tau)$. The resulting model may be written simply as

$$\frac{\partial \eta}{\partial \tau} = y_p(\tau) - \eta \left[1 + \int_{\Lambda_\ell}^{\Lambda_u} e^{-\Lambda^2}(y_\ell^+ + y_\ell^-)\,d\Lambda \right], \tag{25}$$

$$\pm \frac{\partial y_\ell^\pm}{\partial \xi} + \beta \frac{\partial y_\ell^\pm}{\partial \tau} = \gamma \eta e^{-\Lambda^2}(y_\ell^\pm + y_N^\pm) - \alpha' y_\ell^\pm, \tag{26}$$

where α', β, γ, and $y_N^\pm$ are constants. We have taken $\Lambda_\ell = -2$ and $\Lambda_u = 2$ here.

Now consider the boundary conditions. At the left boundary, in terms of the original variables, we have

$$i_\ell^\pm(x = 0, \lambda, t) = R_{10}(1 - R_{11})i_\ell^-(x = 0, \lambda, t) + R_{11}i_\ell^-(x = 0, \lambda + d\lambda_s, t), \tag{27}$$

where $d\lambda_s$ is the Stokes shift. Here R_{11} is a reflectivity function that depends on the total intensity of the left-going laser radiation at the left endpoint,

$$I_L^- = \int_{emband} i_\ell^-(0, \lambda)\,d\lambda \ (\text{W/cm}^2).$$

In terms of the normalized intensity y_ℓ^-, R_{11} is a function $R_{11}(Y_L^-)$ of the normalized total intensity

$$Y_L^- \equiv I_L^-/I_{sat} = \int_{\Lambda_\ell}^{\Lambda_u} y_\ell^-(0, \Lambda)\,d\Lambda, \quad \text{where } I_{sat} \equiv h\nu_0/\sigma_0 t_F, \tag{28}$$

and $\nu_0 = 10^7 c/\lambda_0$ is the center frequency of the laser emission. For this function, we used a model that has been heuristically found [11] to fit well to observations, namely

$$R_{11}(s) = \begin{cases} \frac{s/s_{th} - 1}{s/s_{th} + 6.2} & \text{for } s \geq s_{th} \\ 0 & \text{otherwise,} \end{cases} \tag{29}$$

where s_{th} is a dimensionless constant related to the beam area and the SBS threshold power. Note that the expression (29) neglects the initial turn-on transient. For liquid SBS media, this assumption is justified insofar as the Brillouin scattering lifetime is on the order of 1–2 ns. Thus the left boundary condition (27) can be written

$$y_\ell^+(0, \Lambda) = R_{10}[1 - R_{11}(Y_L^-)]y_\ell^-(0, \Lambda) + R_{11}(Y_L^-)y_\ell^-(0, \Lambda + d\Lambda_s) \quad (\Lambda \leq \Lambda_u - d\Lambda_s)$$

$$y_\ell^+(0, \Lambda_u) = R_{10}[1 - R_{11}(Y_L^-)]y_\ell^-(0, \Lambda_u) \tag{30}$$

for all normalized times τ. In the discretization, we will choose discrete wavelengths such that $\Lambda_{k+1} - \Lambda_k$ exactly equals the nondimensionalized Stokes shift $d\Lambda_s$. Then in the discretized form for (30), where $y_\ell^-(0, \Lambda)$ becomes $y_{0,k}^-$, the shifted value $y_\ell^-(0, \Lambda + d\Lambda_s)$ simply becomes $y_{0,k+1}^-$. The integral defining Y_L^- in (28) is evaluated by means of the trapezoidal rule, as in (7).

The boundary condition at the right end is simply

$$i_\ell^-(x = L_c, \lambda, t) = R_2 i_\ell^+(x = L_c, \lambda, t), \tag{31}$$

which may be written in terms of the normalized quantities as

$$y_\ell^-(1, \Lambda) = R_2 y_\ell^+(1, \Lambda) \tag{32}$$

for all normalized times τ.

The initial conditions that we pose are simply flat zero values at time $\tau = 0$: $\eta(\xi, \tau = 0) = 0$, $y_\ell^+(\xi, \Lambda, \tau = 0) = y_\ell^-(\xi, \Lambda, \tau = 0) = 0$.

To complete the specification of the nondimensionalized problem, we used the following numerical values: $y_p(\tau) = y_{p0} = 0.018$, a constant; $\alpha' = 0.046$; $\beta = 1.35 \times 10^{-4}$; $\gamma = 600$; $y_N^+ = 7.3 \times 10^{-6}$; $y_N^- = 8.8 \times 10^{-7}$; and $s_{th} = 0.073$.

5.2. Solution

The system (25) and (26), together with the boundary equations (30) and (32), clearly fits the general form of the IDE system (1)–(4), with $y_\ell^\pm$, η, ξ, τ, and Λ taking the roles of $y^\pm$, N, x, t, and λ. As detailed in Section 3, we used the method of lines procedure to discretize this system. In both space and wavelength, a uniform grid is appropriate for this problem. We found that $M = 50$ intervals were sufficient to resolve the spatial variation. Our wavelength mesh size was based on the chosen range of ± 1 nm from the center λ_0 of the emission spectrum. Coupled with the Stokes shift of $d\lambda_s = 0.01$ nm, this determines the value $K = 201$ for the number of discrete wavelength points. The corresponding normalized shift is $d\Lambda_s = 0.02$. The integral on the right in Eq. (25) is evaluated using the trapezoidal rule (7). The total size of the resulting ODE system is $N = 20,151$.

We solved the ODE initial value problem with the VODPK solver in the manner described in the preceding sections. We used a preconditioner matrix of product type as shown in (18). Although left or right preconditioning would be equally valid, we chose right preconditioning based on experience with previous problems of this type. In our case, because the spatial mesh is uniform and $v = 1/\beta$ is constant, some simplifications occur in the matrix $\bar{J}_{advec}$ of (20). The two blocks J_m^{1+} and J_m^{1-} are equal, and each block $A_m^{\pm}$ is a scalar matrix, $(\beta \Delta x)^{-1} I$ (a scalar multiple of the $K \times K$ identity matrix). The block B_R is also a scalar matrix, $(R_2/\beta \Delta x) I$, resulting from the simple reflective right boundary condition (32). The block B_L, arising from the Jacobian of the right-hand side of the left boundary condition (30), is actually a full $K \times K$ matrix. However, it is well approximated by the *upper bidiagonal* matrix

$$\bar{B}_L = \frac{1}{\beta \Delta x} \begin{pmatrix} R_{10}(1 - R_{11}) & R_{11} & \\ & \ddots & \ddots \\ & & \ddots \end{pmatrix}, \tag{33}$$

with constant values on the diagonal and superdiagonal. As a result of these features, in the block-LU operations in (23), we do not need to store and save explicitly many of the matrices. Of the matrix blocks shown in (22), we actually store only the $M + 1$ distinct diagonal matrices D_m (overwriting these with their inverses), the bidiagonal matrix $C'_{n-1} = -\gamma D_{2M-1}^{-1} \bar{B}_L$, the diagonal blocks $E_2, \ldots, E_{2M-1}$, and the bidiagonal matrix E_{2M}. From these, the solution of preconditioner linear systems $P_{advec} x = b$ is easily carried out. The storage cost for the entire preconditioner is $6MK + O(M) + O(K)$ (about $3N$) real words.

The equations in this application are sufficiently uncomplicated so that the various Jacobian blocks shown in (15)–(17) and (33) could be evaluated analytically. However, for a more complicated problem, this might not be feasible, and a difference quotient procedure could be used instead.

Once the model representation and the preconditioning were implemented in a Fortran user code, we obtained solutions with VODPK easily. We have run a number of cases, but will show here the results for only one. In what follows, we have used values $R_{10} = 0.4$ and $R_2 = 0.25$.

Figure 2 shows the temporal histories (for the first 150 μs) for the case where the SBS mirror is turned "off," by making s_{th} in Eq. (29) extremely large. The solid curve is the output laser light intensity, defined as $(1 - R_2) I_{sat} \int y_\ell^+ (\xi = 1, \Lambda, \tau) \, d\Lambda$. Also shown in the figure (dashed curve) is the gain coefficient, $g \equiv \sigma_0 N_0 \eta(\xi = 1, \tau) = \sigma_0 N_2(L_c, t)$. In this regime, the laser oscillates solely between the two linear mirrors and the gain coefficient (and the laser intensity as well) exhibit relaxation oscillations (see, for example, [12]). At long times, the system settles down to its steady state, at which the output light intensity is 0.028 MW/cm^2 and the gain coefficient is 0.039 cm^{-1}.

When SBS is turned "on," the temporal histories of the same two variables are as shown in Fig. 3. Note now that the presence of relaxation oscillations has disappeared, and the output consists of a sequence of evenly spaced spikes. Note also that the intensity/spike is roughly a factor of 10 times greater than when SBS is off. Examination of the gain coefficient as a function of time shows that there is greater extraction of the energy in the upper laser level. These characteristics are in agreement with experimentally observed results [13]. With
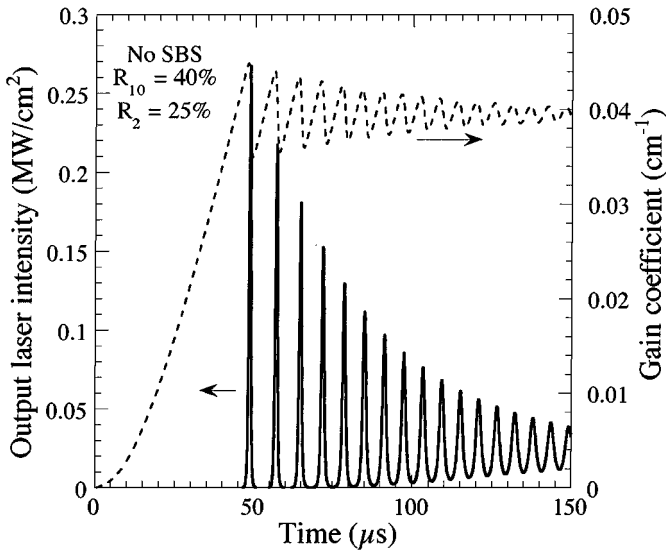
FIG. 2. Laser light history (solid curve) with SBS turned off. The dashed curve is the gain coefficient.

SBS off, there was some residual light in the cavity, as may be seen by the ever-increasing baseline in Fig. 2. With SBS on, there is essentially no light between pulses, as indicated by the zero baseline.

Finally, in Fig. 4 we show, on an expanded time scale, the laser output intensity and gain coefficient for the first pulse in Fig. 3. We see that the FWHM of the pulse is about 240 ns, which is entirely consistent with the amount of energy extraction and the relatively long cavity. The laser model considered in this application assumes oscillation on a single longitudinal mode. Consequently, mode-beating effects (which would show up as oscillations in the pulse of Fig. 4) are absent.
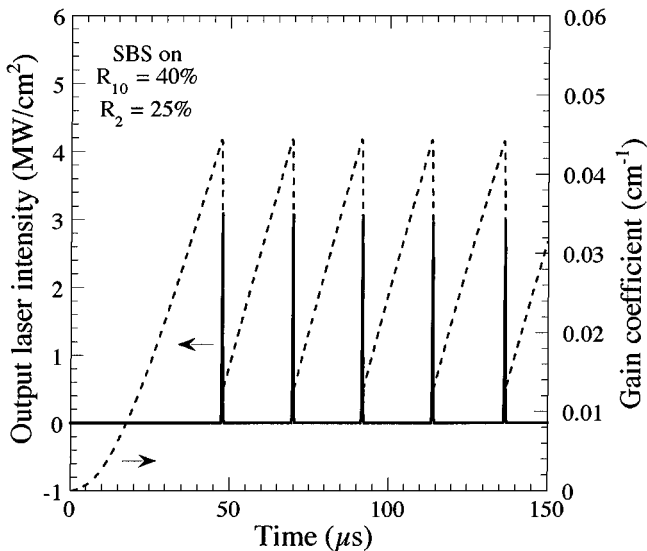
FIG. 3. Laser light history (solid curve) with SBS turned on. The dashed curve is the gain coefficient.
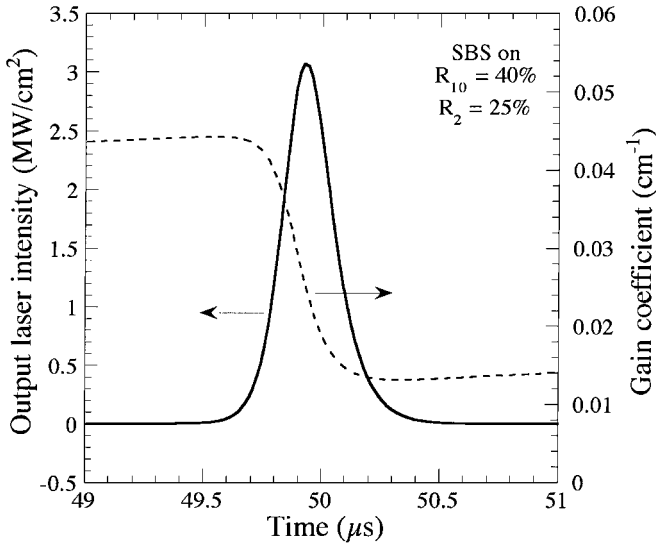
FIG. 4. First SBS pulse on an expanded time scale. The dashed curve is the gain coefficient.

Overall, the VODPK integrator has performed very well on these problems. The case just described, with $M = 50$ and SBS turned on, was integrated to a final time of $t_{final} = 400 \ \mu s$ (final normalized time $\tau_{final} = 5/3$) on a Sun 296 MHz UltraSparc, with a total memory requirement of 8 million double precision words. The performance statistics for this run are shown in Table I, in the column under $M = 50$. The step count NST may seem high, but was fully appropriate for the accurate resolution of the laser oscillations. The average number of Newton iterations per step (NNI/NST) and of linear iterations per Newton iteration (NLI/NNI) were both only slightly larger than one, and each preconditioner evaluation lasted an average of 7.9 steps (NST/NPE). These figures indicate that the BDF integration method is performing very well and that the quality of the preconditioner is extremely high.

If one doubles the mesh size to $M = 100$, the solution does not change significantly; the statistics are given in the last column of Table I. For this case, the average number of Newton iterations per step (NNI/NST) and of linear iterations per Newton iteration (NLI/NNI) remain about the same as for $M = 50$. However, the number of steps per preconditioner evaluation (NST/NPE) increased from 7.9 to 8.7.

The presence of periodic fine structure in the time history of the solution might suggest that the problem may not really be stiff. To settle this question, we made a run for the

TABLE I
Performance Statistics for SBS Model with Two Mesh Sizes

Mesh size M	50	100
NST = no. time steps	4535	5631
NFE = no. evaluations of right-hand side function F	12,364	15,020
NPE = no. evaluations of preconditioner P	573	648
NNI = no. nonlinear (Newton) iterations	5487	6724
NLI = no. linear (SPGMR) iterations	6873	8292
NPS = no. preconditioner linear system solves	11,706	14,251
CPU time	4.96 min	13.5 min

case $M = 50$ with the nonstiff method option in VODPK. This uses variable-order Adams–Moulton methods, and involves no linear algebra. This run took 878 min on the same machine (177 times that of the stiff method run), 1,540,920 steps (340 times higher), and 2,923,419 F evaluations (236 times higher). The average cost of a nonstiff step is lower than that of a stiff step, but only by a factor of about $340/177 = 1.9$ (attesting to the effectiveness and efficiency of the preconditioned iterative method). Outweighing this is the restriction on step sizes forced by stiffness ($t_{final}/NST \approx 0.26$ ns), which raises the total cost for the nonstiff method far above that of the stiff method.

6. CONCLUSIONS

We have shown how a simple extension of the Method of Lines may be used to solve a certain class of IDE systems. The success of this method lies in the choice of an efficient ODE solver to handle the (usually stiff) system of ODEs. Emphasis has been placed on the formation of the preconditioner in product form, the use of which greatly improves the efficiency of the ODE solver. The spectral integral in the problem has its impact in the second preconditioner factor, which consists of bordered-diagonal matrices.

The philosophy behind the product preconditioner is similar to that in operator splitting (or fractional step) approaches to time-dependent problems, wherein each fractional step involves only a part of the problem. The difference here is that the approximation of the Newton matrix A by the product P is done within a Krylov iteration for the solution of a linear system, within a Newton iteration for a nonlinear system, within an integration time step, and each of these three iteration levels involves a convergence test to control the errors being committed. In contrast, traditional operator splitting involves no iteration and no error control. Certainly, other choices for the product preconditioner are possible, using different splittings of the Jacobian, or using more than two factors. However, because of the success we have had with the present choice, we have not explored alternatives.

Besides the application presented in the previous section, other areas of laser physics that can be addressed with the same solution methodology include mirrorless lasers, amplification of broadband laser radiation, and gain-switched laser oscillators. It would be easy to extend the solution approach to systems with multiple population variables; the bordered-diagonal matrices would then have borders wider than one, but an analogous LU solution could still be used. It would also be easy to extend the approach to bidirectional IDE systems in two space dimensions. This would increase the problem size and expand the preconditioner factor based on the advection terms, but would not alter the basic methodology.

APPENDIX

Nondimensionalization of Laser Equations

Let us define a dimensionless wavelength

$$\Lambda = \sqrt{4 \ln 2}(\lambda - \lambda_0)/\Delta\lambda;$$

then the integral in (24) is

$$\int_{emband} = \frac{\Delta\lambda^2 \sigma_0}{4 \ln 2} \int_{\Lambda_\ell}^{\Lambda_u} \left(\Lambda + \frac{\sqrt{4 \ln 2}\lambda_0}{\Delta\lambda} \right) e^{-\Lambda^2} (i_\ell^+ + i_\ell^-) \, d\Lambda.$$

Since $\Delta\lambda$ is so small, for any reasonable integration range, the second term in parentheses will dominate. Thus we take

$$\int_{emband} = \frac{\Delta\lambda\sigma_0}{\sqrt{4\ln 2}}\lambda_0 \int_{\Lambda_\ell}^{\Lambda_u} e^{-\Lambda^2}(i_\ell^+ + i_\ell^-)\, d\Lambda.$$

If we now define a spectral saturation intensity

$$i_{sat} = \frac{hc\sqrt{4\ln 2}\cdot 10^7}{\sigma_0\lambda_0 t_F \Delta\lambda} = \frac{\sqrt{4\ln 2}}{\Delta\lambda}I_{sat}\ (\text{W/cm}^2 - \text{nm}),$$

and define scaled intensities by $y_\ell^\pm \equiv i_\ell^\pm/i_{sat}$, then the rate equation may be written

$$\frac{\partial N_2}{\partial t} = \frac{\sigma_a N_0 I_p(t)}{h\nu_p} - \frac{N_2}{t_F}\left[1 + \int_{\Lambda_\ell}^{\Lambda_u} e^{-\Lambda^2}(y_\ell^+ + y_\ell^-)\, d\Lambda\right].$$

If we define

$$I_{p,sat} = \frac{h\nu_p}{\sigma_a t_F}$$

and the dimensionless variables

$$\tau \equiv t/t_F, \quad \eta \equiv N_2/N_0, \quad \text{and} \quad y_p \equiv I_p/I_{p,sat},$$

then the first of Eqs. (24) may be written

$$\frac{\partial\eta}{\partial\tau} = y_p(\tau) - \eta\left[1 + \int_{\Lambda_\ell}^{\Lambda_u} e^{-\Lambda^2}(y_\ell^+ + y_\ell^-)\, d\Lambda\right]. \tag{34}$$

Now look at the transport equation, the second of Eqs. (24). Divide both sides by i_{sat}, and write

$$\xi \equiv x/L_c, \quad \gamma \equiv \sigma_0 N_0 L_a, \quad \alpha' \equiv \alpha L_a, \quad \beta \equiv nL_c/ct_F.$$

Then the transport equation may be written

$$\pm\frac{\partial y_\ell^\pm}{\partial\xi} + \beta\frac{\partial y_\ell^\pm}{\partial\tau} = \gamma\eta e^{-\Lambda^2}(y_\ell^\pm + y_N^\pm) - \alpha' y_\ell^\pm, \tag{35}$$

where $y_N^\pm$ is the (normalized) noise source $i_N^\pm/i_{sat}$. Equations (34) and (35) are the normalized equivalent of Eqs. (24).

ACKNOWLEDGMENTS

REFERENCES

1. N. K. Madsen and R. F. Sincovec, The numerical Method of Lines for the solution of nonlinear partial differential equations, in *Computational Methods in Nonlinear Mechanics*, edited by J. T. Oden *et al.* (Texas Institute for Computational Mechanics, University of Texas at Austin, 1974), p. 371.

2. E. I-Ho Lin and J. L. Sackman, Identification of the dynamic properties of nonlinear vicoelastic materials and the associated wave propagation problem, *Int. J. Solids Struct.* **11**(10), 1145 (1975).

3. G. D. Byrne, Pragmatic experiments with Krylov methods in the stiff ODE setting, in *Computational Ordinary Differential Equations*, edited by J. R. Cash and I. Gladwell (Oxford University Press, Oxford, 1992), p. 323.

4. P. N. Brown, G. D. Byrne, and A. C. Hindmarsh, VODE, a variable-coefficient ODE solver, *SIAM J. Sci. Stat. Comput.* **10**(5), 1038 (1989).

5. Y. Saad and M. H. Schultz, GMRES: A generalized minimal residual algorithm for solving nonsymmetric linear systems, *SIAM J. Sci. Stat. Comput.* **7**(3), 856 (1986).

6. P. N. Brown and A. C. Hindmarsh, Reduced storage matrix methods in stiff ODE systems, *J. Appl. Math. Comp.* **31**(5), 40 (1989).

7. R. A. Fisher, Ed., *Optical Phase Conjugation* (Academic Press, New York, 1983), pp. 465–535.

8. M. Gower and D. Proch, Eds., *Optical Phase Conjugation* (Springer-Verlag, Berlin, 1994), pp. 288–313.

9. A. Koechner, *Solid-State Laser Engineering,* 4th ed. (Springer-Verlag, Berlin, 1996).

10. A. A. Kaminskii, *Laser Crystals—Their Physics and Properties* (Springer-Verlag, Berlin, 1990).

11. B. Dane, Private communication (1999).

12. A. Siegman, *Lasers* (University Science Books, Mill Valley, CA, 1986), Ch. 13.

13. M. Ostermeyer, A. Heuer, and R. Menzel, 27-W average output power with 1.2*DL beam quality from a single-rod Nd: YAG laser with phase-conjugating SBS mirror, *IEEE J. Quantum Electron.* **34**, 372 (1998).